



# Genotoxic effects and transcriptional deregulation of genetic biomarkers in *Chironomus riparius* larvae exposed to hydroxyl- and amine-terminated generation 3 (G3) polyamidoamine (PAMAM) dendrimers



Rosario Planelló<sup>a</sup>, Roberto Rosal<sup>b</sup>, Mónica Aquilino<sup>a</sup>, Óscar Herrero<sup>a,\*</sup>

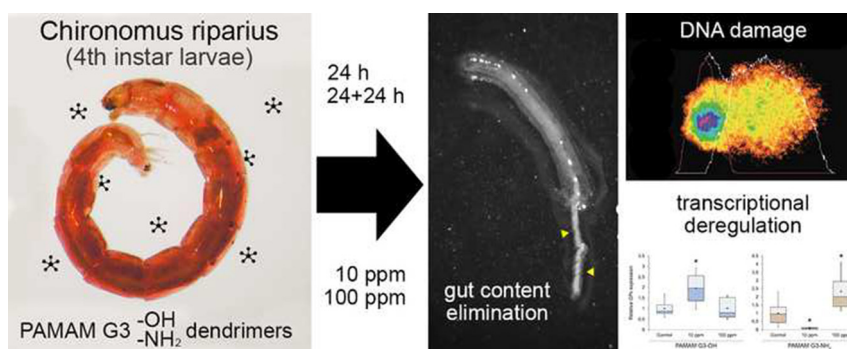
<sup>a</sup> Grupo de Biología y Toxicología Ambiental, Facultad de Ciencias, Universidad Nacional de Educación a Distancia (UNED), E-28040 Madrid, Spain

<sup>b</sup> Departamento de Ingeniería Química, Universidad de Alcalá, Alcalá de Henares, Madrid, Spain

## HIGHLIGHTS

- The toxicity of PAMAM G3 dendrimers was assessed in *Chironomus riparius* larvae.
- Larvae exposure to PAMAM G3-NH<sub>2</sub> dendrimers led to gut content elimination.
- Hydroxyl- and amine-terminated dendrimers were able to alter gene transcription.
- PAMAM G3 dendrimers may alter the regular activity of hormonal nuclear receptors.
- DNA damage caused by G3-OH and G3-NH<sub>2</sub> dendrimers was detected using the comet assay.

## GRAPHICAL ABSTRACT



## ARTICLE INFO

### Article history:

Received 29 October 2020

Received in revised form 22 January 2021

Accepted 8 February 2021

Available online xxxxx

Editor: Daniel Wunderlin

### Keywords:

PAMAM dendrimers  
Gene expression  
Comet assay  
Endocrine disruption  
Genotoxicity  
Ecotoxicity

## ABSTRACT

The physical-chemical properties of polyamidoamine (PAMAM) dendrimers give them attractive qualities for multiple applications, including biomedical purposes. Their use has significantly increased in recent years, and there is currently a lack of information on their potential adverse effects on biological systems, which raises particular concerns about the risks to human health and the environment from their use and disposal. Studies focusing on ecotoxicological effects are particularly scarce. In the present work, we have used the model insect *Chironomus riparius* to assess the toxicity of hydroxyl-terminated and amine-terminated generation 3 PAMAM dendrimers: PAMAM G3-OH and PAMAM G3-NH<sub>2</sub>. Fourth-instar larvae were exposed to 10 or 100 ppm G3-OH or G3-NH<sub>2</sub> dendrimers for 24 h (acute toxicity) or 24 + 24 h (delayed toxicity). Using quantitative real-time PCR, we analyzed transcriptional alterations in genes related to relevant physiological pathways: *EcR*, *GAPDH*, *GPx*, *GST*, *hsp10*, *hsp24*, *Gp93*, and *rpl4*. We also used the comet assay to assess the possible genotoxic characteristics of the dendrimers and their ability to induce DNA breakage. Regarding the effects on transcriptional activity, our results showed that G3-NH<sub>2</sub> dendrimers induced greater (and in many cases opposite) alterations than G3-OH dendrimers, especially in acute 24-hour exposures. Delayed toxicity studies showed that both dendrimers produced transcriptional alterations even 24 h after the withdrawal of the compound and frequently contrary to what was observed acutely. In both cases, the lowest concentration studied (10 ppm) was the most toxic. On the other hand, the comet assay allowed us to detect genotoxic effects for the two dendrimers, thus demonstrating their ability to interact with DNA. This work provides new information about the possible

\* Corresponding author.

E-mail address: [oscar.herrero@ccia.uned.es](mailto:oscar.herrero@ccia.uned.es) (Ó. Herrero).

disruptive effects of PAMAM G3 dendrimers on the health of exposed organisms, alerting the need to carry out more studies to deepen their toxic characteristics and mode of action, especially in natural environments.

© 2021 Elsevier B.V. All rights reserved.

## 1. Introduction

PAMAM (polyamidoamine) dendrimers are one of the most attractive molecules for biomedical applications. Their use as drug and gene/DNA delivery systems improves the efficacy and safety of chemical drugs or biological agents. Besides, their versatility has paved the way for its potential use in numerous areas including cosmetics (e.g., hair-styling gels, shampoos, sunscreens, and anti-acne products), printing technologies (e.g., inkjet cartridges, toners), the textile industry (e.g., water repellent coatings), and the painting industry (e.g., varnish) (Bodewein et al., 2016).

They are nanoscopic polymeric molecules with multiple amidoamine branched monomers (dendrons) that emanate from a central ethylenediamine core (Mintzer and Grinstaff, 2011). In the manufacturing process, dendrimers are grown off the central core giving rise to a new generation (G) with each step. Their surface can be polymerized or modified with peripheral functional groups, and both the core and the branching units determine the dendrimer morphology. Thus, while low-number generations exhibit almost linear geometries, later generations show more globular-like shapes (Araújo et al., 2018). Generations also determine their physicochemical properties. In this regard, their high polarity decreases as generation increases, and high generation (4 or more) PAMAM dendrimers have relatively high gene transfection efficacy with demonstrated cytotoxicity in vivo and in vitro. In contrast, low generation (0 to 3) dendrimers diminish their transfection effectiveness and are nearly no cytotoxic (Li et al., 2018).

Along with their increasingly widespread use, the specific properties of dendrimers raise concerns about adverse effects on biological systems and pose an increased risk to humans and the environment. Considering the wide range of proposed applications of PAMAM dendrimers, there is an urgent need to study the human- and environmental-related toxicity of these dendritic polymer nanoparticles to ensure their efficient assessment in order to avoid adverse effects (OECD, 2010; Naha et al., 2018). The endpoints proposed by the OECD for environmental toxicology studies of nanomaterials include effects on microorganisms, soil species, pelagic species, and also sediment species such as *Chironomus riparius*, the insect species used in this work. It should be noted that current analytical techniques do not allow the quantification of dendrimers in the range of environmental concentrations found for other micropollutants, so to date, there is a serious lack of information about the levels of dendrimers in the environment (Ulaszewska et al., 2012; Santiago-Morales et al., 2014).

Cytotoxicity detected in mammalian cell lines has been primarily associated with the increased production of reactive oxygen species (ROS) at higher generations (Janaszewska et al., 2012; Kunzmann et al., 2011). Given their ability to interact and destabilize cell membranes, their terminal groups also play an essential role in their toxicity, being the cationic dendrimers more toxic than the neutral ones (Bodewein et al., 2016; Jain et al., 2010; Mecke et al., 2005).

Few studies have demonstrated the toxicity of dendrimers in ecotoxicologically relevant species: the bacteria *Vibrio fischeri* (Mortimer et al., 2008; Naha et al., 2009), the cyanobacterium *Anabaena* sp. (Gonzalo et al., 2015; Tamayo-Belda et al., 2019), the algae *Chlamydomonas reinhardtii* (Gonzalo et al., 2015; Petit et al., 2010), and the crustaceans *Daphnia magna* or *Thamnocephalus platyurus* (Naha et al., 2009). The zebrafish model has been used to evaluate mortality (Calienni et al., 2017; Pryor et al., 2014), physiological alterations (Bodewein et al., 2016), developmental toxicity (Heiden et al., 2007), and teratogenicity (Calienni et al., 2017), among other endpoints (Martinez et al., 2017, and references therein) in higher trophic levels.

It also has been shown that PAMAM dendrimers can alter the transcriptional profile of cell lines (Feliu et al., 2015) and organisms like *C. reinhardtii* (Petit et al., 2012), *Caenorhabditis elegans* (Walczynska et al., 2018) or zebrafish embryos (Oliveira et al., 2014). However, information about the toxic environmental effects of PAMAM dendrimers is still very scarce, and therefore the potential risks to humans and ecosystems are still difficult to evaluate.

Among all insect species used in ecotoxicological studies, the aquatic midge *C. riparius* has four standardized OECD protocols for the evaluation of water and sediment toxicity (OECD, 2004), and it is widely used given its ecological relevance and its ubiquitous presence worldwide in almost any aquatic environment. Apart from traditional life-cycle toxicity endpoints (e.g., survival, development, reproduction), molecular approaches to assess early toxic effects through changes in gene expression or enzymatic activity have gained high relevance in the last decade. Thus, among other studies, this organism has demonstrated to be useful for the early detection of toxic molecular effects after exposure to metals (Planelló et al., 2010), plasticizers (Herrero et al., 2014, 2015), endocrine disruptors (Herrero et al., 2018) or chemical mixtures (Arambourou et al., 2019), even in natural populations (Planelló et al., 2015b).

In the present work, we have used fourth instar larvae of *C. riparius* to assess time and dose toxic effects of neutral (hydroxyl-terminated) and cationic (amine-terminated) third-generation polyamidoamine dendrimers. Through quantitative real-time PCR, we have analyzed variations in the transcriptional activity of genes related to the ecdysone hormonal pathway (ecdysone receptor: *Ecr*), the detoxification (glutathione peroxidase: *GPx*; glutathione S-transferase: *GST*) and the energy (glyceraldehyde-3-phosphate dehydrogenase: *GAPDH*) metabolisms, the cellular stress response (heat-shock proteins 10 and 24: *hsp10*, *hsp24*; glycoprotein 93: *Gp93*) and the ribosomal biogenesis (ribosomal protein L4: *rpL4*). We have also used the comet assay as a first approach to investigate the genotoxic effects of these molecules, their ability to induce DNA breaks.

## 2. Material and methods

### 2.1. Characterization of dendrimers

Third generation hydroxyl- and amine-terminated poly(amidoamine) dendrimers with ethylenediamine core (PAMAM G3) were purchased from Dendritech (Midland, MI, USA). Hydroxyl-terminated (G3-OH) and amine-terminated (G3-NH<sub>2</sub>) were purchased with a concentration of 15.9 wt% and 9.43 wt% respectively in water from Dendritech. The test solution, 100 ppm (14.4 μM for G3-OH and 14.5 μM for G3-NH<sub>2</sub>), was prepared using ultrapure water from a Direct-Q™ 5 Ultrapure Water Systems (Millipore, Bedford, MA, USA) with a specific resistance of 18.2 MΩ cm. Nanoparticle size distributions were obtained using dynamic light scattering (DLS) (Table 1) in a Malvern Zetasizer Nano ZS equipment (Malvern Instruments Ltd., Worcestershire, UK). Zeta-potential measurements were performed at 25 °C in pure water at the prescribed without any modification using electrophoretic light scattering combined with phase analysis light scattering in the same Zetasizer Nano ZS instrument.

### 2.2. Test animals

The experimental animals were aquatic larvae from the non-biting midge *C. riparius*. Stock cultures are routinely maintained in our laboratory following standardized guidelines (OECD, 2011), under constant

**Table 1**

Dynamic light scattering hydrodynamic size and  $\zeta$ -potential determined by electrophoretic light scattering with 95% confidence intervals (pH 6.5).

Dendrimer	Assay	DLS size (nm)	$\zeta$ -potential (mV)
G3-OH	Pure water	223 ± 37	+9.4 ± 1.0
	100 ppm (14.4 µM)	3.48 ± 0.35	
	Culture medium	205 ± 25	-1.5 ± 1.0
	100 ppm	4.10 ± 0.62	
	After 24 h exposure	538 ± 71	-17.3 ± 1.3
	10 ppm		
	After 24 + 24 h exposure	773 ± 210	-15.4 ± 0.9
	10 ppm		
	After 24 h exposure	743 ± 83	-16.8 ± 1.2
	100 ppm		
G3-NH <sub>2</sub>	After 24 + 24 h exposure	559 ± 78	-18.8 ± 1.4
	100 ppm		
	Pure water	219 ± 22	+26.5 ± 2.8
	100 ppm (14.5 µM)	3.98 ± 0.24	
	Culture medium	183 ± 14	+3.9 ± 0.6
	100 ppm	4.21 ± 0.42	
	After 24 h exposure	680 ± 123	-1.42 ± 0.18
	10 ppm		
	After 24 + 24 h exposure	493 ± 90	-16.7 ± 1.5
	10 ppm		
-	After 24 h exposure	1352 ± 259	-1.37 ± 0.14
	100 ppm		
	After 24 + 24 h exposure	1492 ± 271	-15.8 ± 1.3
	100 ppm		
	Culture medium (fresh)	153 ± 17	-6.3 ± 0.8
-	Control 24 h	505 ± 72	-18.0 ± 0.9
	Control 48 h	308 ± 48	-16.2 ± 1.1

aeration at 20 °C and standard light:dark photoperiod (16 L:8D). Larvae are grown from egg masses in polyethylene tanks containing aqueous culture medium (0.5 mM CaCl<sub>2</sub>, 1 mM NaCl, 1 mM MgSO<sub>4</sub>, 0.1 mM NaHCO<sub>3</sub>, 0.025 mM KH<sub>2</sub>PO<sub>4</sub>, and 0.01 mM FeCl<sub>3</sub>), supplemented with nettle leaves, commercial fish food (TetraMin®, Tetra, Germany), and cellulose tissue. Experiments were carried out using exclusively fourth instar larvae from different stock cultures (to promote genetic variability), and the larval stage was determined based on the size of the head capsule (USEPA, 2000).

### 2.3. Exposure conditions

Stock aqueous solutions of both G3-OH and G3-NH<sub>2</sub> PAMAM dendrimers were prepared in *C. riparius* culture medium, at the initial concentration of 1000 ppm, and were diluted in fresh medium to obtain the desired test concentrations: 10 and 100 ppm. The experimental design included two exposure times: 24-h continuous exposure (acute toxicity; 24 h); and 24-h exposure followed by an additional 24-h in fresh culture medium (delayed toxicity; 24 + 24 h). Six independent experiments were performed. For each dose (control, 10 ppm, or 100 ppm) and time (24 h or 24 + 24 h) dendrimer experimental condition, twenty-five fourth instar larvae were exposed to 50 mL of the testing solution in 150 mL glass vessels (height: 8 cm, diameter: 6 cm). After exposure, survival rates were calculated for each experimental condition (n = 150) and a group of five surviving larvae randomly selected from each vessel were stored in an Eppendorf tube at -80 °C until subsequent RNA extraction for qPCR analyses (total larvae = 30; n = 6). Larvae eliminating the gut content were photographed using a trinocular Nikon SMZ-2T stereomicroscope (Nikon, Japan) with a CCD Photometrics® CoolSNAP™ digital camera (Photometrics, USA).

### 2.4. RNA isolation and cDNA synthesis

Total RNA was extracted from frozen larvae using TRIzol® Reagent (Invitrogen, Carlsbad, CA, USA) following the manufacturer's protocol. Samples were then treated with RNase-free DNase (Roche, Germany) for 90 min, and an organic extraction with phenol-chloroform was

completed using Phase Lock Gel™ Light tubes (5Prime, Germany) to optimize aqueous phase recovery. RNA was precipitated using isopropyl alcohol (0.5 v/v), then washed with 70% ethanol and resuspended in DEPC water. The quality and quantity of total RNA were determined by absorption spectroscopy in a BioPhotometer® 6131 equipment (Eppendorf, Germany). Purified RNA was stored at -80 °C. Reverse transcription was performed with 0.5 µg of the isolated RNA and 100 units of M-MLV RT enzyme (Invitrogen) in the presence of 0.5 µg oligo (dT)<sub>20</sub> primer (Invitrogen) and 0.5 µM dNTPs (Biotools, Spain) at 37 °C for 50 min in a reaction volume of 20 µL.

### 2.5. Quantitative real-time PCR

The cDNA obtained was used as the template for the Polymerase Chain Reaction (PCR). Quantitative real-time PCR (qPCR) was used to evaluate the mRNA expression profile of *Ecr*, *GAPDH*, *Gp93*, *Gpx*, *GST*, *hsp10*, *hsp24*, and *rpL4* genes, and was performed using a CFX96™ Real-Time PCR Detection System (Bio-Rad, Hercules, CA, USA) and the SsoFast™ EvaGreen® Supermix (Bio-Rad). Genes encoding actin and the ribosomal subunit 26S were used as endogenous reference controls (Planelló et al., 2015a). The statistical validation of the stability of the reference genes was performed using CFX Manager™ 3.1 software (Bio-Rad), using an iterative test for pairwise variation, according to Vandesompele et al. (2002). Primer sequences and efficiencies are shown in Table 2. The qPCR was run using the following cycling conditions: 30 s initial denaturation at 95 °C, 39 cycles of 5 s denaturation at 95 °C, 15 s annealing at 58 °C, and 10 s elongation at 65 °C. Amplification efficiencies and correlation coefficients for each primer pair were calculated as described in Bio-Rad's Real-Time PCR Applications Guide (catalog #170-9799). For all genes, the efficiency of the assay was among 90–105% (R<sub>2</sub> > 0.980). A melting curve analysis was performed after amplification to verify the accuracy of each amplicon. CFX Manager™ 3.1 software was used to determine total mRNA levels by normalizing the expression (2<sup>-ΔC<sub>q</sub></sup>) of the target genes against the two endogenous reference genes. Each sample was run in duplicate wells, and three independent replicates were performed for each experimental condition.

### 2.6. Comet assay

Measurement of DNA damage was performed using a single cell gel electrophoresis assay (SCGE), following the OxiSelect™ Comet Assay Kit (Cell Biolabs, USA) protocol. For each experimental condition, twelve fourth-instar larvae were placed on a fine mesh strainer (0.3 mm mesh), which was laid over a mortar containing 3 mL of cold 1× phosphate-buffered saline (PBS). Since the larvae have a hard exoskeleton, several transverse cuts were made with a scalpel to facilitate the extraction of the cells. A pestle was used to gently grind up the sample and get the cell suspension, avoiding the presence of cuticle debris as much as possible. Mechanical mincing was carried out with the sample immersed in ice-cold PBS to avoid cell damage caused by the oxidation of the sample in contact with air. The sample was then carefully homogenized by pipetting and transferred into a 1.5 mL Eppendorf tube (on ice).

The homogenate was centrifuged for 5 min at 4 °C and 1500 rpm, and the pellet was resuspended in 250 µL of cold 1× PBS. From each cell suspension (1 × 10<sup>4</sup> cells/mL), 10 µL were mixed with 100 µL of molten OxiSelect™ Comet Agarose, and 75 µL of this mix were immediately transferred onto the OxiSelect™ Comet Slide, ensuring complete good coverage. The slides were maintained horizontally and transferred to 4 °C in the dark for 1 h. The cells were then treated with the lysis buffer (1 h at 4 °C in the dark; pH 10) and the alkaline solution (30 min at 4 °C in the dark; pH > 13), following the manufacturer's instructions. After that, the slides were transferred to a horizontal electrophoresis chamber and exposed to an electric field of 1 V/cm and 300 mA for 20 min in a cold TBE electrophoresis solution (300 mM NaOH, 1 mM EDTA; pH > 13). After the alkaline electrophoresis, the slides were washed

**Table 2**

Primers used for quantitative real-time PCR analysis in *C. riparius* fourth-instar larvae. Forward and reverse DNA primer sequences are provided for both the housekeeping genes (26S and actin) and the target genes.

Gene	Forward (5'-3')	Reverse (5'-3')
26S	TTCGCGACCTCAACTCATGT	CCGCATTCAAGCTGGACTTA
actin	GATGAAGATCCTACCGAACC	CGGAAACGTTTCATTACCG
EcR	TCTTCTACGGCCATCGTCA	GCTGCATCTTGTTCCGCA
GAPDH	GGTATTTCAATGAATGATCACTTTG	TAATCCTTGGATTGCATGTACTTG
Gp93	TGCCGTTTTGAGATCAGGCT	TCCTCTCGTCAGTCTGTTCTG
GpX	AAGTGTGGTTACACAGCTAAGCATT	GATATCCAAATTGATTACACGGAAA
GST	TGGTTGAAACGAGAGACCA	TCGGATATAGTAGTCCAGCATCG
hsp10	GGAGATCAAGTCTCTTGGCT	TTTCGCGAGGATATCGCCTT
hsp24	TCACTTAATGACTGGATATCG	GAATCCATCTTGCCGAAATGC
rpL4	AACGCTCAGAGCTGGACGTGG	ATTATCTTGTGTACGCTCATTG

three times in dH<sub>2</sub>O for 5 min, and then in 70% ethanol for 5 min. Finally, slides were air-dried, stained for 15 min with 100 µL/well of diluted Vista Green DNA Dye (Cell Biolabs, USA), and observed in a Zeiss Axiophot Photomicroscope (Zeiss, Germany) with a FITC filter, and coupled to a CCD Photometrics® CoolSNAP™ digital camera.

For each well, at least fifty cells were randomly photographed and analyzed using the CometScore 2.0 software (Tritek Corp., USA), which provides data for the following genotoxicity parameters: comet length, comet height, comet area, comet intensity, comet mean intensity, head diameter, head area, head intensity, head mean intensity, % DNA in head, tail length, tail area, tail intensity, tail mean intensity, % DNA in tail, tail moment, and olive moment. According to the literature (Liao et al., 2009), two of these parameters were selected as representative of genotoxic damage: the percentage of DNA in the tail (which is directly proportional to the percentage of DNA damage that has occurred in a particular cell), and tail moment (defined as the percentage of DNA in the tail multiplied by the tail length).

### 2.7. Data analysis

Data normality and homoscedasticity were checked using the Shapiro–Wilk and Levene tests, respectively. Normally distributed data were analyzed with ANOVA, followed by Bonferroni or Games-Howell post hoc tests, when appropriate. Non-normal data were analyzed with the nonparametric Kruskal–Wallis test, and the differences between pairs (treatments) were established using Mann–Whitney *U* tests. *p* values below 0.05 were considered statistically significant: \* (*p* ≤ 0.05), \*\* (*p* ≤ 0.01), \*\*\* (*p* ≤ 0.001), \*\*\*\* (*p* ≤ 0.0001). Statistical analyses were performed using the software Prism 8.2.1 (GraphPad Software, USA).

## 3. Results

### 3.1. Physicochemical characteristics of PAMAM dendrimers

The DLS hydrodynamic size and the ζ-potential of hydroxyl- and amine-terminated PAMAM G3 dendrimers were determined under the different experimental conditions (Table 1). The charge of dendrimers, measured as ζ-potential was positive at high concentrations due to the protonation of terminal primary amines in the case of G3-NH<sub>2</sub>, while in the case of G3-OH the positive charge can be attributed to the weaker protonation of internal tertiary amines (Buczowski et al., 2016). In culture medium, we observed slightly negatively charged aggregates displaying sizes in the 150–500 nm range. The hydrodynamic size distribution of dendrimers dispersed in water and culture medium at high concentration clearly showed two peaks, one of them about 4 nm, which agreed well with the molecular size of G3 as provided by the manufacturer. All dendrimer dispersions presented aggregates in the hundreds of nanometers range that increased with time and reached micron size ranges for G3-NH<sub>2</sub> after 24 and 24 + 24 h.

### 3.2. Survival test

No effects were observed on the exposed *C. riparius* fourth instar larvae. Neither neutral nor cationic dendrimers affected the survival of the larvae, in any of the experimental conditions (dose and time) tested. The highest mortality rates were detected in the delayed toxicity experiments (24 + 24 h) at 10 ppm PAMAM G3-OH (3.7%) and 10 ppm G3-NH<sub>2</sub> (6.25%), although they were not statistically significant.

### 3.3. Physiological effects

Larvae exposed to 100 ppm PAMAM G3-NH<sub>2</sub> showed a clear physiological effect, consisting of eliminating their gut content enclosed in the peritrophic matrix (Fig. 1). Compared to control larvae, this effect was statistically significant and observed in 50.0% (±2.3) of larvae in acute 24-hour exposures (*n* = 150; *p* < 0.0001), and also in 45.7% (±8.7) of larvae maintained 24 h after the dendrimer withdrawal (24 + 24 h) (*n* = 147; *p* = 0.0063). No significant differences were found between these two exposure conditions. This physiological effect was not observed in any other experimental condition.

### 3.4. Transcriptional alterations

The transcriptional profile of different genes of interest under the selected experimental conditions was analyzed through quantitative real-time PCR. In this regard, fourth-instar *C. riparius* larvae were exposed to 10 and 100 ppm of PAMAM G3-OH and G3-NH<sub>2</sub> dendrimers in acute (24-h exposure) and delayed (24-h exposure plus additional 24-h in fresh culture medium) toxicity studies.

As an overview, in the case of hydroxyl-terminated dendrimers, the genes *EcR* (Fig. 2A and B), and *GST* (Fig. 2G and H) showed no significant alterations in any of the experimental conditions, neither in the 24-hour tests nor in the 24 + 24-hour tests. In these dendrimers, the highest concentration tested (100 ppm) did not affect the genes studied at any of the exposure times. On the contrary, all genes were altered to some extent after exposure to the amino-terminated dendrimers, particularly in the lowest concentration (10 ppm).

Five genes suffered a significant increase in their expression levels in the case of larvae exposed to 10 ppm G3-OH for 24 h: *GpX* (2-fold; *p* = 0.036) (Fig. 2E), *hsp10* (4-fold; *p* = 0.0044) (Fig. 3A), *hsp24* (3.7-fold; *p* = 0.0192) (Fig. 3C), *Gp93* (6.9-fold; *p* = 0.0312) (Fig. 3E), and *rpL4* (5.1-fold; *p* = 0.0075) (Fig. 3G). The removal of the dendrimer led to the overexpression of some genes when in the first 24 h they had shown no effect (as is the case with *GAPDH* (2.6-fold; *p* = 0.011) (Fig. 2D)), or to maintaining the acute effect detected in the first 24 h (as *GpX* (1.9-fold; not significant) (Fig. 2F)). Differently, other genes were significantly repressed at 24 + 24 h, when in the previous 24 h they showed an overexpression effect: *hsp10* (0.2-fold; *p* = 0.038) (Fig. 3B), *hsp24* (0.1-fold; *p* = 0.004) (Fig. 3D), and *rpL4* (0.4-fold; not significant) (Fig. 3H).

*EcR* was significantly downregulated (0.3-fold; *p* = 0.008) after 24-hour exposure to 10 ppm G3-NH<sub>2</sub> (Fig. 2A), while dendrimer withdrawal (Fig. 2B) led to strong overexpression (up to 9-fold; *p* = 0.004). These effects were similar in other genes, with acute repressions in *GAPDH* (0.3-fold; *p* = 0.012) (Fig. 2C), *GpX* (0.1-fold; *p* = 0.0002) (Fig. 2E), *GST* (0.1-fold; *p* = 0.0002) (Fig. 2G), *hsp10* (0.2-fold; *p* = 0.0095) (Fig. 3A), *hsp24* (0.1-fold; *p* = 0.0003) (Fig. 3C), and *rpL4* (0.8-fold; not significant) (Fig. 3G), followed by delayed overexpressions: *GAPDH* (5.7-fold; *p* = 0.0091) (Fig. 2D), *GpX* (8.6-fold; *p* = 0.0011) (Fig. 2F), *GST* (3.1-fold; *p* = 0.004) (Fig. 2H), *hsp10* (4-fold; *p* = 0.0051) (Fig. 3B), *hsp24* (6.6-fold; *p* = 0.0087) (Fig. 3D), and *rpL4* (25.9-fold; *p* = 0.0095) (Fig. 3H). For *Gp93*, although acute repression was also detected (0.2-fold; 0.0002) (Fig. 3E), the effect continued (0.7-fold; not significant) after removing the cationic dendrimer (Fig. 3F).

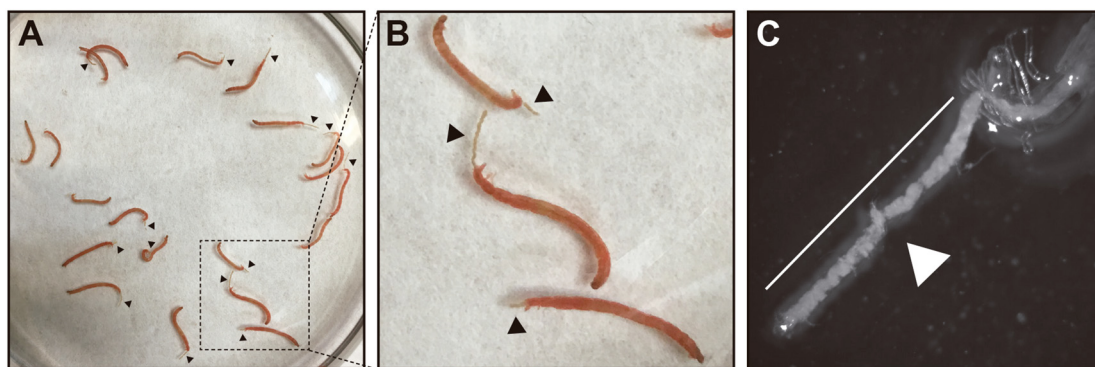


**Fig. 1.** Elimination of the gut content in *C. riparius* fourth-instar larvae exposed to 100 ppm G3-NH<sub>2</sub> PAMAM dendrimers for 24 h. (A) Black arrowheads indicate individuals eliminating their gut content. (B) Enlarged zoom area. (C) Detailed view of the gut content (white arrowhead) coming out of the anal lobe and covered by the peritrophic matrix.

While exposures to 10 ppm NH<sub>2</sub> led to generalized repression after 24 h, 24-hour assays with 100 ppm NH<sub>2</sub> showed an evident overexpression in the case of *EcR* (2.2-fold;  $p = 0.0081$ ) (Fig. 2A), *GAPDH* (4.2-fold;  $p = 0.001$ ) (Fig. 2C), *GPx* (2.3-fold;  $p = 0.0297$ ) (Fig. 2E), and *hsp10* (2.7-fold;  $p = 0.0238$ ) (Fig. 3A). On the contrary, and following the same tendency detected for the lowest dose, the highest one also caused significant downregulation of *hsp24* (0.3-fold;  $p = 0.0005$ ) (Fig. 3C), and *Gp93* (0.4-fold;  $p = 0.004$ ) (Fig. 3E). No effects were detected in the delayed toxicity studies with 100 ppm NH<sub>2</sub> in any of the genes analyzed.

Taking into account all the results obtained by qPCR, Fig. 4 summarizes all the alterations in the transcriptional activity of the genes studied, according to the different experimental conditions tested with both PAMAM G3-OH and G3-NH<sub>2</sub> dendrimers. In a general overview, the cationic (G3-NH<sub>2</sub>) dendrimers showed stronger and more significant effects on gene expression levels than the neutral (G3-OH) ones. Moreover, concerning the concentrations tested, the lowest dose was also the one with the most remarkable effects in both dendrimers.

### 3.5. DNA damage

The comet assay allowed us to identify differences in genotoxic effects induced by the two dendrimers studied. As shown in Fig. 5, both dendrimers were able to induce DNA damage at 24-hour exposures at the two doses tested (10 and 100 ppm). G3-OH produced a significant increase in DNA breaks, reflected by both the %DNA in tail (Fig. 5A) (1.42-fold at 10 ppm;  $p = 0.004$ ) (1.35-fold at 100 ppm;  $p = 0.0018$ ), and the tail moment (Fig. 5B) (2.43-fold at 10 ppm;  $p < 0.0001$ ) (2.35-fold at 100 ppm;  $p < 0.0001$ ). In contrast, both parameters reflected values below the control levels in exposures to G3-NH<sub>2</sub>: % DNA in tail (Fig. 5C) (0.93-fold at 10 ppm; not significant) (0.7-fold at 100 ppm;  $p = 0.0002$ ), and tail moment (Fig. 5D) (0.71-fold at 10 ppm; not significant) (0.47-fold at 100 ppm;  $p = 0.0001$ ).

## 4. Discussion

Although cellular toxic effects of exposure to dendrimers have been assessed in recent years, especially in *in vitro* studies, there is currently a significant lack of knowledge about the ecotoxicity that these molecules can produce in ecosystems when released into different environmental compartments. Since dendrimers have proven to be very useful tools in a wide range of biomedical applications (e.g., drug targeting, gene delivery, antimicrobial and antiviral activities, analgesic and anti-inflammatory properties, tissue engineering, or transfection, among others) (Araújo et al., 2018; Mintzer and Grinstaff, 2011; Naha et al., 2018), their use has been spreading worldwide. This fact is reflected by the notable increase in the number of publications on these molecules that have arisen in the last two decades (Janaszewska et al., 2019). The ultimate disposal of these molecules into the environment,

mainly through wastewater systems, may lead to their entry into the food chains and affect non-target organisms. Taking into account this possible effect on water environments, we have selected for this work an insect species that is widely represented throughout the planet in aquatic ecosystems. In this sense, *C. riparius*, together with other chironomids, constitutes a recognized model in ecotoxicology studies (OECD, 2004; Taenzler et al., 2007; USEPA, 2000), and adults and larvae of this species exposed to a great number of environmental stressors have proved to be useful biomarkers of toxicity (Boros and Ostafe, 2020; Mantilla et al., 2017; Planelló et al., 2020; Zhang et al., 2020; and references therein).

PAMAM hydroxyl- and amine-terminated dendrimers represent two different classes of terminal group functionalization. The surface charge of G3-NH<sub>2</sub>, measured as  $\zeta$ -potential, was positive due to the protonation of terminal primary amines ( $pK_a = 6.3$ – $6.7$ ) while G3-OH was essentially neutral, the slightly positive charge observed at high concentration being attributed to the weaker protonation of internal tertiary amines ( $pK_a = 9$ – $9.9$ ) (Buczkowski et al., 2016). DLS measurements performed at 100 ppm ( $\sim 14 \mu\text{M}$ ) in pure water allowed measuring a peak in the 3.5–4.0 nm range, which represented a low percentage of the intensity signal, but dominant in Mie's number distributions. These peaks corresponded to the expected size of the dendrimer molecules (Kavyani et al., 2014). In culture medium, only the broader signal from aggregates could be appreciated due to the relatively low sensitivity of DLS for PAMAM dendrimers. The limitation is a consequence of the little difference in the refractive index of dendrimers and water (Chu, 2008). Under these circumstances, the dendrimer appeared as a monodisperse solution with a diameter of aggregates in the few hundreds of nanometer range (183 and 205 nm for G3-NH<sub>2</sub> and G3-OH respectively in freshly prepared solutions). Most probably, individual dendrimers and aggregates coexist in a dynamic equilibrium. The higher size of aggregates in the case of G3-NH<sub>2</sub> dendrimers may be explained by heteroaggregation with the negatively charged particles of the background colloid.

It was previously shown that both amine- and hydroxyl-terminated dendrimers significantly enhanced the formation of intracellular reactive oxygen species (Gonzalo et al., 2015; Naha et al., 2018). It could be proved that cell damage was linked to mitochondria and caused cytoplasm disorganization, membrane disruption, and cell death. Amine-terminated dendrimers were internalized by algae and cyanobacteria, and the similarity in the damage produced suggested that both kinds of dendrimers, cationic and non-cationic, share a similar mode of action (Gonzalo et al., 2015; Tamayo-Belda et al., 2019). To assess possible similarities or differences between the effects of G3-OH and G3-NH<sub>2</sub> dendrimers, in our work with *C. riparius*, we have assessed at the molecular level their toxicity by studying the transcriptional responses of eight biomarker genes and also evaluating DNA damage in exposed larvae.



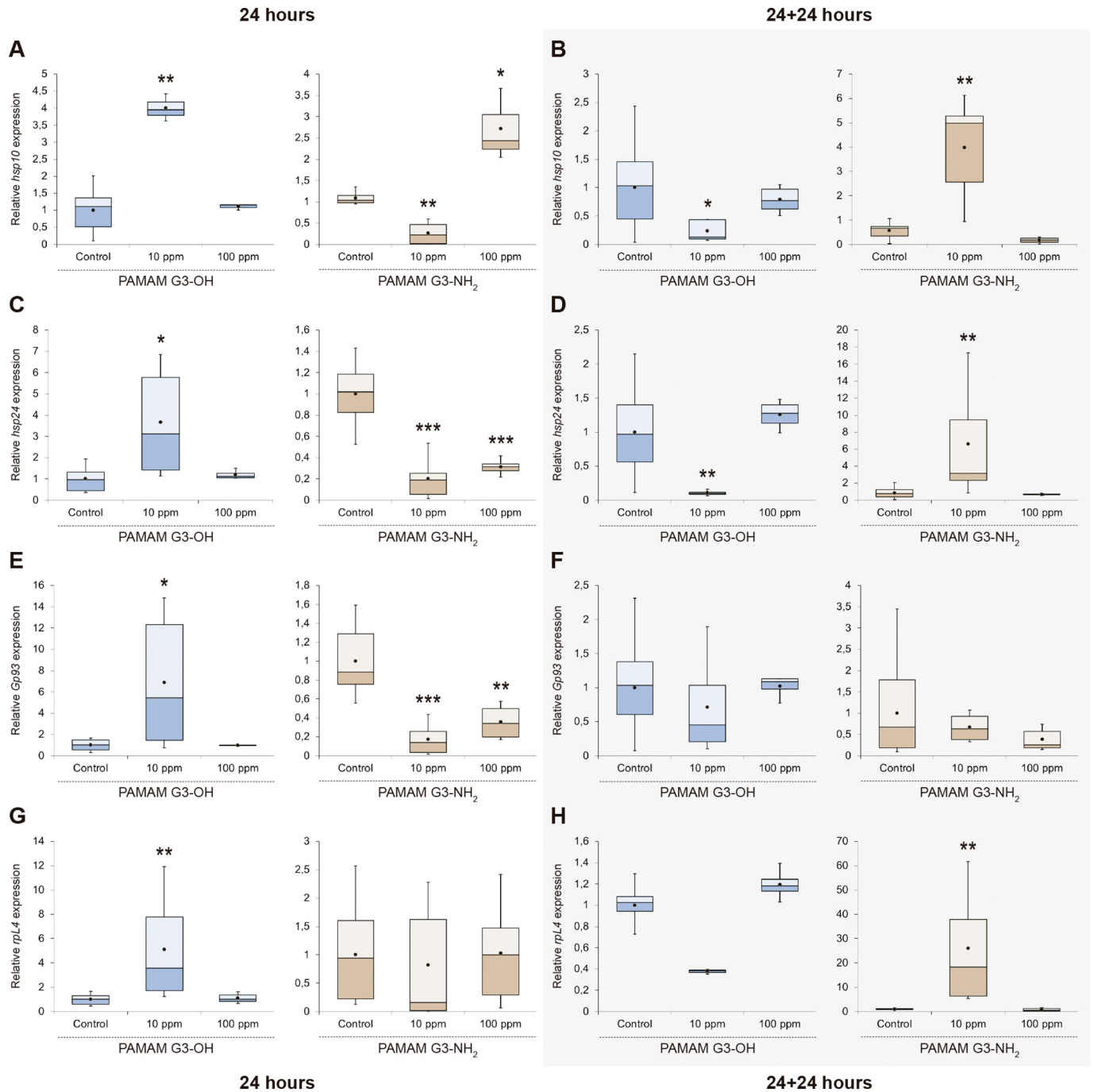


**Fig. 3.** Transcriptional activity of *hsp10*, *hsp24*, *Gp93* and *rpL4* in *C. riparius* fourth-instar larvae exposed to 10 or 100 ppm G3-OH (blue boxes) or G3-NH<sub>2</sub> (orange boxes) PAMAM dendrimers for 24 h (acute toxicity; white background; A, C, E, G) or 24 + 24 h (delayed toxicity; grey background; B, D, F, H). Asterisks indicate significant differences with respect to the control values: \* ( $p \leq 0.05$ ), \*\* ( $p \leq 0.01$ ), \*\*\* ( $p \leq 0.001$ ). (For interpretation of the references to color in this figure legend, the reader is referred to the web version of this article.)

peritrophic matrix was associated with the disturbed structural organization of the midgut (Procópio et al., 2015). This mechanism has been reported as a defense mechanism by which the mosquito larvae aim to excrete unabsorbed harmful compounds, constituting an adaptive response (Abedi and Brown, 1961; Gusmão et al., 2002). However, it should be noted that this is a rare physiological response in *C. riparius*, as it has so far not been described in the abundant scientific literature focusing on the toxic effects on this species of a wide variety of biotic and abiotic factors, including xenobiotics.

Under these sublethal conditions, a set of gene biomarkers were selected to assess early toxic effects in *C. riparius*. The gene encoding the

ecdysone receptor (*Ecr*) constitutes the starting point of this hormonal pathway's genetic cascade. In insects, the coordinated response of the genes involved in this cascade is crucial in developmental processes that regulate growth, molting, and metamorphosis (Planelló et al., 2015a; Truman, 2019). *GAPDH* encodes the glyceraldehyde-3-phosphate dehydrogenase and has been commonly used as a reference housekeeping gene in qPCR studies. This enzyme plays a key role in the glycolytic pathway, but other numerous functions have been described in a diverse range of cellular processes (Nicholls et al., 2012). *GPx* and *GST* encode two antioxidant enzymes: glutathione peroxidase (GPx) and glutathione S-transferase (GST). While GPx catalyzes the reduction

	3G-OH		3G-NH <sub>2</sub>	
	10 ppm	100 ppm	10 ppm	100 ppm
24h	<i>EcR</i>	<i>EcR</i>	<i>EcR</i> **	<i>EcR</i> **
	<i>GAPDH</i>	<i>GAPDH</i>	<i>GAPDH</i> *	<i>GAPDH</i> ***
	<i>GPx</i> *	<i>GPx</i>	<i>GPx</i> ***	<i>GPx</i> *
	<i>GST</i>	<i>GST</i>	<i>GST</i> ***	<i>GST</i>
	<i>hsp10</i> **	<i>hsp10</i>	<i>hsp10</i> **	<i>hsp10</i> *
	<i>hsp24</i> *	<i>hsp24</i>	<i>hsp24</i> ***	<i>hsp24</i> ***
	<i>Gp93</i> *	<i>Gp93</i>	<i>Gp93</i> ***	<i>Gp93</i> **
	<i>rpL4</i> **	<i>rpL4</i>	<i>rpL4</i>	<i>rpL4</i>
24+24h	<i>EcR</i>	<i>EcR</i>	<i>EcR</i> **	<i>EcR</i>
	<i>GAPDH</i> *	<i>GAPDH</i>	<i>GAPDH</i> **	<i>GAPDH</i>
	<i>GPx</i>	<i>GPx</i>	<i>GPx</i> **	<i>GPx</i>
	<i>GST</i>	<i>GST</i>	<i>GST</i> **	<i>GST</i>
	<i>hsp10</i> *	<i>hsp10</i>	<i>hsp10</i> **	<i>hsp10</i>
	<i>hsp24</i> **	<i>hsp24</i>	<i>hsp24</i> **	<i>hsp24</i>
	<i>Gp93</i>	<i>Gp93</i>	<i>Gp93</i>	<i>Gp93</i>
	<i>rpL4</i>	<i>rpL4</i>	<i>rpL4</i> **	<i>rpL4</i>

**Legend (fold change):**

> 1 → 5	0.5 → < 1
> 5 → 10	0.1 → < 0.5
> 10	< 0.1

**Fig. 4.** Colormap scheme of the down- and up-regulation effects caused in *C. riparius* 4th instar larvae exposed to 10 or 100 ppm G3-OH or G3-NH<sub>2</sub> PAMAM dendrimers for 24 h (acute toxicity) or 24 + 24 h (delayed toxicity). Changes in gene expression measured by quantitative real-time PCR are presented with a color pattern based on fold-change with respect to the control values. Asterisks indicate significant differences with respect to the control values: \* ( $p \leq 0.05$ ), \*\* ( $p \leq 0.01$ ), \*\*\* ( $p \leq 0.001$ ).

of hydrogen peroxide to water and oxygen, GST is a multifunctional phase II biotransformation enzyme that makes xenobiotics more water-soluble substances, facilitating their excretion (de Melo et al., 2020). Both enzymes are of great importance for the survival of organisms since they modulate their activity in response to the presence of reactive oxygen species (ROS) and enable adaptive responses to the oxidative stress they cause. Heat shock proteins (HSPs) act as intracellular chaperones, and their main function is to correct unfolded or misfolded proteins to keep cell normal function. HSPs are synthesized constitutively in insects and induced by stressors such as heat, cold, crowding, and anoxia (King and MacRae, 2015). In particular, Hsp10 is a mitochondrion-resident protein involved in mitochondrial protein import and macromolecular assembly, but it can also be found in the cytosol and extracellularly (David et al., 2013). On the other hand, Hsp24 is a cytoplasmic small heat shock protein (sHSP) whose functions, together with those intrinsic to chaperones, are involved in stress response, development, and inhibition of apoptosis (Martín-Folgar et al., 2015). Gp93, the endoplasmic reticulum paralog of Hsp90, is a chaperone involved in various biological processes, among which, in addition to protein folding, are the midgut development and the endodermal digestive tract morphogenesis (Maynard et al., 2010). Finally, rpL4 encodes for the ribosomal protein L4, which, together with other ribosomal proteins (RPs), is implied in ribosome biogenesis, and thus indispensable for the proper functioning of the protein synthesis machinery (Herrero et al., 2016).

An overview of the results obtained in this work shows that PAMAM G3-NH<sub>2</sub> dendrimers (strongly cationic) produced stronger and more

significant transcriptional alterations than G3-OH dendrimers (neutral), especially in acute 24-hour exposures (Fig. 4). This fact is consistent with their greater ability to interact with (negatively charged) biomembranes, leading them to trigger toxic effects by disrupting the cell wall (Clogston and Patri, 2011; Janaszewska et al., 2019). Many studies have revealed that cationic PAMAM dendrimers can cross cell membranes by various endocytic pathways, although dendrimers' cellular internalization and trafficking depend on their size, shape, charge, surface functionality, and cell type (Uram et al., 2015). The small size of third-generation PAMAM dendrimers, 30–70 Å (Buczkowski et al., 2016), allows them to reach the interior of the nucleus. Although there is no evidence that this type of nanoparticles interferes with the endocrine function (Lu et al., 2013), their characteristics open up the possibility that PAMAM G3 dendrimers may alter the regular activity of hormonal nuclear receptors (NRs) or interact with their associated hormones.

The downregulation detected in the *EcR* transcriptional levels after 24 h of exposure to 10 ppm G3-NH<sub>2</sub> dendrimers (Fig. 2A) showed a clear ecdysone antagonistic activity. After removing the nanoparticles from the culture medium, we observed the opposite effect, with the dendrimers mimicking the natural hormone's effect and triggering the upregulation of the gene that encodes its receptor (Fig. 2B). This differential response may be due to a physiological adaptation in which the larvae neutralize the initial acute damage, trying to recover this hormonal pathway's normal functioning. These effects have also been observed after exposure to xenobiotics (Herrero et al., 2018), and in the present work confirms the ability of PAMAM G3-NH<sub>2</sub> dendrimers to

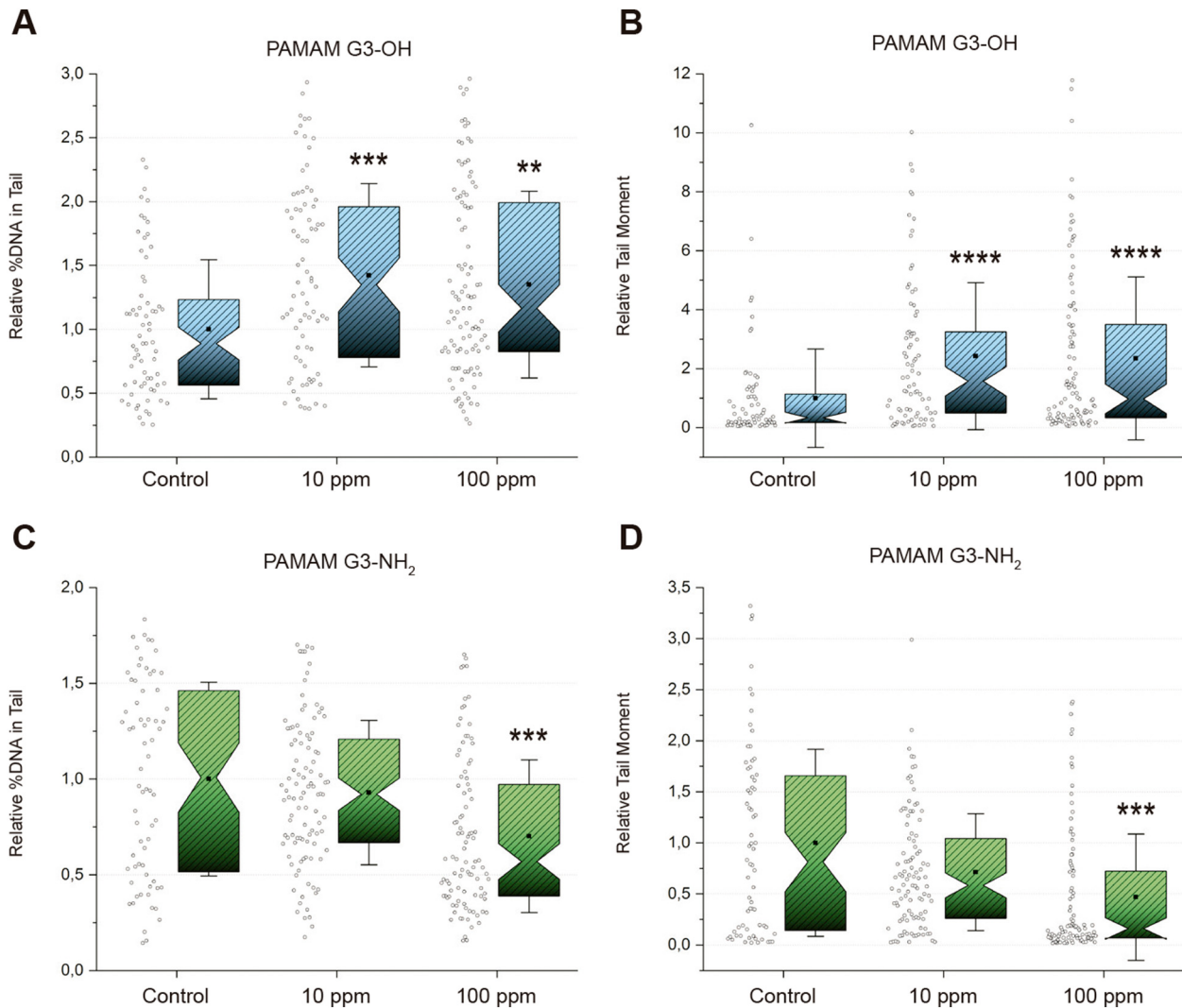


**Fig. 5.** DNA damage induced in *C. riparius* fourth-instar larvae after exposure to 10 or 100 ppm of PAMAM G3-OH (blue boxes) and G3-NH<sub>2</sub> (green boxes) dendrimers during 24 h. Results obtained from three independent experiments (12 individuals for each experimental condition) are expressed as % DNA in tail and relative tail moment. Asterisks indicate significant differences with respect to the control values: \*\* ( $p \leq 0.01$ ), \*\*\* ( $p \leq 0.001$ ), \*\*\*\* ( $p \leq 0.0001$ ). (For interpretation of the references to color in this figure legend, the reader is referred to the web version of this article.)

disrupt the endocrine function. Future studies evaluating the effect after longer exposures, such as full life cycle or multigenerational experiments, will help assess the mode of action of PAMAM dendrimers on the endocrine system of insects and how these nano-polymeric structures may affect the viability of their populations.

Similarities found in the transcriptional responses of the studied genes may attend to an overall effect on the gene activity of the exposed larvae. In this regard, 10 ppm of both cationic and neutral dendrimers were able to alter the transcriptional activity of *GAPDH* (Fig. 2C and D), a gene that is presumed to be stable and frequently used as a suitable loading control in gene expression studies. Nevertheless, only the cationic ones altered this gene activity at 100 ppm (Fig. 2C), with a significant upregulation after acute 24-hour exposures. It is worth noting the significant increase in *GAPDH* expression in recovery studies (24 + 24 h), 24 h after the removal of the dendrimers from the culture medium. Although it is currently known that this enzyme is involved in multiple biological functions (Nicholls et al., 2012; Tristan et al., 2011), its implication in the energy metabolism is decisive, and its greater or lesser activity can modulate the general metabolic status of the organism.

That physiological wellness is also conditioned by the organism's ability to adapt to changing environmental conditions, where several

detoxification pathways come into play. The ability of PAMAM dendrimers to alter various enzyme activities has been previously described. In an in vitro study, both neutral and cationic dendrimers were able to inhibit the activity of the enzyme pepsin (Ciolkowski et al., 2013). In another work with dendrimers with hydroxyl terminal groups, the interaction of these nano molecules with different ATPases led to the inhibition of these enzymes, also showing that this effect decreased when higher concentrations of dendrimers were used (Ciolkowski et al., 2011). In the present work, both PAMAM G3-OH and G3-NH<sub>2</sub> dendrimers altered the expression levels of *Gpx* in acute 24-hour exposures (Fig. 2E), while *GST* was only significantly affected by G3-NH<sub>2</sub> dendrimers (Fig. 2G). Our results show that 10 ppm/24-hours with the neutral dendrimers activated the transcription of *Gpx*, which could affect the cytosolic route that catalyzes the reduction of hydrogen peroxide and peroxide radicals. On the other side, cationic dendrimers strongly repressed this detoxification pathway under the same exposure conditions. 10 ppm G3-NH<sub>2</sub> also repressed the transcriptional activity of *GST*, which could affect the catalytic activity of the enzyme and its protective role against electrophilic reagents. The effect with 100 ppm G3-NH<sub>2</sub>/24 h was opposite to that observed at 10 ppm, with significant activation of *Gpx* or no effect on *GST*. Both dendrimers caused similar expression patterns 24 h after their removal

from the culture medium (Fig. 2F and H). While 100 ppm did not seem to affect either *Gpx* or *GST*, 10 ppm led to a clear overexpression of both genes, significant for G3-NH<sub>2</sub> dendrimers. Thus, it seems that despite G3-OH removal, both *Gpx* and *GST* tended to remain overexpressed, while after the withdrawal of G3-NH<sub>2</sub> the larvae turned the initial repression into increased transcriptional activity. Therefore, the ability of PAMAM dendrimers to alter the transcription of genes that encode for different biotransformation and detoxification enzymes can seriously compromise the proper functioning of these metabolic pathways and, therefore, the adaptive capacity of exposed organisms.

Acting as mediators in protein-protein interactions, collaborating in their proper folding (shape), and preventing the formation of unwanted protein aggregates, the role of HSPs as chaperones is crucial in maintaining the organisms' homeostasis and triggering adaptive responses to environmental stress (Chen et al., 2018; King and MacRae, 2015). In addition, many other functions have been described in the case of sHSPs, being involved in stress tolerance, cell death, differentiation, cell cycle, signal transduction, and development, among others (Bakthisaran et al., 2015). Their regulation occurs primarily at the level of transcription, but in some cases (e.g., *Drosophila melanogaster*), it appears to be independent of heat shock transcription factors (HSFs) and dependent on steroid hormones (Solary and Garrido, 2002).

To date, no studies have been conducted on the alterations that exposure to dendrimers can cause on the normal activity of HSPs. Mainly due to the oxidative stress that these nano molecules can induce, toxic effects have been described in vitro in different cell lines (Janaszewska et al., 2019; Mukherjee et al., 2010a; Naha et al., 2009), and in vivo in bacteria (Naha et al., 2009), cyanobacteria (Gonzalo et al., 2015), green algae (Gonzalo et al., 2015; Petit et al., 2012; Suarez et al., 2011), plants (Fernández Freire et al., 2015), crustaceans (Naha et al., 2009), and fish (Bodewein et al., 2016; Calienni et al., 2017; Heiden et al., 2007). In the present work with *C. riparius* *hsp10*, *hsp24*, and *Gp93* transcriptional activities were altered after PAMAM dendrimer exposure (Fig. 3). Again, the most significant effects in 24-hour treatments (Fig. 3A, C, and E) were triggered by the presence of G3-NH<sub>2</sub> dendrimers in the culture medium, which in general strongly reduced the normal transcriptional levels of these genes (with the exception of *hsp10*, which was slightly overexpressed at 100 ppm). In the recovery studies (24 + 24 h), only the lowest concentration studied (10 ppm) showed an effect on *hsp10* (Fig. 3B) and *hsp24* (Fig. 3D) after the removal of the nano molecules. These genes reduced their transcriptional activity due to G3-OH dendrimers but increased it by G3-NH<sub>2</sub>. *Gp93* remained unaffected in these delayed toxicity studies (Fig. 3F). It is worth mentioning that the evaluated dendrimers were able to affect the activity of genes that encode for proteins of different biological compartments: cytoplasm, mitochondria, and endoplasmic reticulum. Thus, their final effect on the organism would derive not only from their described capacity to destabilize the integrity of the cellular membranes but also from altering the correct functioning of the machinery they contain. This is particularly relevant in the case of mitochondria since the destabilization of this organelle can further promote the release of ROS, as the electron transport chain is considered as their major natural source.

The stability in the transcriptional activity of *rpL4* after 24-hour exposure to PAMAM G3-NH<sub>2</sub> dendrimers contrasted with the multiple alterations detected in the other genes studied. Since ribosomal biogenesis is crucial for the cellular translation machinery, the synthesis of ribosomal proteins is a fairly well-preserved process (Herrero et al., 2016). In the present study, the inalterability of *rpL4* activity could indicate that the effects on other genes are not due to a global affectation of transcriptional processes, but to specific alterations derived from exposure to PAMAM dendrimers.

Finally, after verifying that PAMAM dendrimers could affect DNA at the transcriptional level, we studied their possible genotoxic effects using the comet assay, a sensitive and rapid technique for quantifying and analyzing DNA damage in individual cells (Azqueta and Collins, 2013). Few previous studies have demonstrated the ability

of these nanomaterials to produce DNA damage. In vitro works with different cell lines linked this effect with ROS production, which also led to the appearance of oxidative stress and apoptosis (Choi et al., 2010; Mukherjee et al., 2010b; Naha and Byrne, 2013). Another toxicological assessment was carried out using the *Allium cepa* test (Fernández Freire et al., 2015), a recognized higher plant model used to evaluate DNA damages (such as chromosome aberrations and disturbances in the mitotic cycle) that can ultimately lead to DNA fragmentation. In the present work, both exposures to PAMAM G3-OH and G3-NH<sub>2</sub> dendrimers produced a significant effect on DNA damage rates, although in opposite ways. While hydroxyl-terminated dendrimers induced a significant increase in the %DNA in tail at 10 ppm and 100 ppm (Fig. 5A and B), under the same experimental conditions, the amino-terminated dendrimers showed an anti-genotoxic effect, with values below those obtained in the controls (Fig. 5C and D). Since it has been proven that PAMAM dendrimers could induce genotoxic damage, including chromosomal bridges (Fernández Freire et al., 2015), this decrease in the %DNA in tail values may be due to the presence of DNA cross links. The comet assay is hampered by cross linking because it prevents the relaxation and extension of DNA loops under electrophoresis (Azqueta et al., 2013). For both dendrimers, the effects were dose-dependent. In a previous study with *A. aegypti*, disorganization of larval midgut epithelium, similar to that observed in this work with *C. riparius* under PAMAM G3-NH<sub>2</sub> exposure, was associated with DNA damage/fragmentation (Procópio et al., 2015). Considering those results, we would have expected in our research that *C. riparius* larvae exposed to G3-NH<sub>2</sub> dendrimers would have reflected the most significant genotoxic damage. In contrast, in our experiments, exposure to G3-OH dendrimers showed the highest genotoxicity values, although without visible midgut alterations. These results highlight the disparities in the toxic effects of dendrimers on DNA integrity and highlight the need for further research into the mode of action of these molecules.

## 5. Conclusions

This is the first time that the possible toxic effects of PAMAM dendrimers have been studied in an insect model. Previous studies have demonstrated these nano molecules' ability to induce toxicity mainly through oxidative damage by generating reactive oxygen species. Although the mechanisms underlying the observed effects have not been studied in this work, the exposure to dendrimers significantly altered the transcriptional activity of the selected genes, and genotoxic damage was also detected in the exposed larvae. While in the transcriptional studies, the most remarkable effects were detected for G3-NH<sub>2</sub> dendrimers, in the case of DNA damage, the G3-OH dendrimers showed the most significant effect. The differences in the effects of amino- and hydroxyl-terminated PAMAM dendrimers were also reflected by the occurrence of physiological changes in the former (elimination of gut content), while for the latter, no apparent effects were observed. This work provides new and valuable information about the possible environmental implications of exposure to PAMAM dendrimers, and further studies will be necessary to assess the risk derived from their presence in natural ecosystems.

## CRedit authorship contribution statement

**Rosario Planelló:** Funding acquisition, Investigation, Methodology, Writing – review & editing. **Roberto Rosal:** Investigation, Methodology, Writing – review & editing. **Mónica Aquilino:** Investigation, Software, Writing – review & editing. **Óscar Herrero:** Conceptualization, Data curation, Funding acquisition, Investigation, Methodology, Software, Supervision, Visualization, Writing – original draft, Writing – review & editing.

## Declaration of competing interest

The authors declare that they have no known competing financial interests or personal relationships that could have appeared to influence the work reported in this paper.

## Acknowledgements

This research was supported by the Universidad Nacional de Educación a Distancia (UNED); Independent Thinking grant for young researchers within the Plan for the Promotion of Research and Internationalization (2018); grant in the Call for University Cooperation and Sustainable Development Goals (2018-PUNED-0006). Mónica Aquilino was awarded a postdoctoral contract (PEJD-2019-POST/AMB-16425) co-financed by UNED and the Government of the Community of Madrid.

## References

- Abedi, Z.H., Brown, A.W.A., 1961. Peritrophic membrane as vehicle for DDT and DDE excretion in *Aedes aegypti* larvae. *Ann. Entomol. Soc. Am.* 54, 539–542. <https://doi.org/10.1093/aesa/54.4.539>.
- Arambourou, H., Planelló, R., Llorente, L., Fuertes, I., Barata, C., Delorme, N., Noury, P., Herrero, Ó., Villeneuve, A., Bonneau, C., 2019. *Chironomus riparius* exposure to field-collected contaminated sediments: from subcellular effect to whole-organism response. *Sci. Total Environ.* 671, 874–882. <https://doi.org/10.1016/j.scitotenv.2019.03.384>.
- Araújo, R., Santos, S., Igne Ferreira, E., Giarolla, J., 2018. New advances in general biomedical applications of PAMAM dendrimers. *Molecules* 23, 2849. <https://doi.org/10.3390/molecules23112849>.
- Azqueta, A., Collins, A.R., 2013. The essential comet assay: a comprehensive guide to measuring DNA damage and repair. *Arch. Toxicol.* 87, 949–968. <https://doi.org/10.1007/s00204-013-1070-0>.
- Azqueta, A., Arbillaga, L., Lopez de Cerain, A., Collins, A., 2013. Enhancing the sensitivity of the comet assay as a genotoxicity test, by combining it with bacterial repair enzyme FPG. *Mutagenesis* 28, 271–277. <https://doi.org/10.1093/mutage/get002>.
- Bakthisaran, R., Tangirala, R., Rao, C.M., 2015. Small heat shock proteins: role in cellular functions and pathology. *Biochim. Biophys. Acta* 1854, 291–319. <https://doi.org/10.1016/j.bbapap.2014.12.019>.
- Bodewein, L., Schmelter, F., Di Fiore, S., Hollert, H., Fischer, R., Fenske, M., 2016. Differences in toxicity of anionic and cationic PAMAM and PPI dendrimers in zebrafish embryos and cancer cell lines. *Toxicol. Appl. Pharmacol.* 305, 83–92. <https://doi.org/10.1016/j.taap.2016.06.008>.
- Evaluation of Ecotoxicology Assessment Methods of Nanomaterials and Their Effects. In: Boros, B.-V., Ostafe, V. (Eds.), *Nanomater.* (Basel, Switzerland) 10, 610. <https://doi.org/10.3390/nano10040610>.
- Buczowski, A., Waliszewski, D., Urbaniak, P., Palecz, B., 2016. Study of the interactions of PAMAM G3-NH2 and G3-OH dendrimers with 5-fluorouracil in aqueous solutions. *Int. J. Pharm.* 505, 1–13. <https://doi.org/10.1016/j.ijpharm.2016.03.061>.
- Calienni, M.N., Feas, D.A., Igartúa, D.E., Chiamoni, N.S., Alonso, S. del V., Prieto, M.J., 2017. Nanotoxicological and teratogenic effects: a linkage between dendrimer surface charge and zebrafish developmental stages. *Toxicol. Appl. Pharmacol.* 337, 1–11. <https://doi.org/10.1016/j.taap.2017.10.003>.
- Chen, B., Feder, M.E., Kang, L., 2018. Evolution of heat-shock protein expression underlying adaptive responses to environmental stress. *Mol. Ecol.* <https://doi.org/10.1111/mec.14769>.
- Choi, Y.J., Kang, S.J., Kim, Y.J., Lim, Y., Chung, H.W., 2010. Comparative studies on the genotoxicity and cytotoxicity of polymeric gene carriers polyethyleneimine (PEI) and polyamidoamine (PAMAM) dendrimer in Jurkat T-cells. *Drug Chem. Toxicol.* 33, 357–366. <https://doi.org/10.3109/01480540903493507>.
- Chu, B., 2008. Dynamic light scattering. In: Borsali, R., Pecora, R. (Eds.), *Soft Matter Characterization*. Springer Netherlands, Dordrecht, pp. 335–372. [https://doi.org/10.1007/978-1-4020-4465-6\\_7](https://doi.org/10.1007/978-1-4020-4465-6_7).
- Ciolkowski, M., Rozanek, M., Szewczyk, M., Klajnert, B., Bryszewska, M., 2011. The influence of PAMAM-OH dendrimers on the activity of human erythrocytes ATPases. *Biochim. Biophys. Acta Biomembr.* 1808, 2714–2723. <https://doi.org/10.1016/j.bbame.2011.07.021>.
- Ciolkowski, M., Rozanek, M., Bryszewska, M., Klajnert, B., 2013. The influence of PAMAM dendrimers surface groups on their interaction with porcine pepsin. *Biochim. Biophys. Acta Protein Proteomics* 1834, 1982–1987. <https://doi.org/10.1016/j.bbapap.2013.06.020>.
- Clogston, J.D., Patri, A.K., 2011. Zeta potential measurement. In: McNeil, S. (Ed.), *Methods in Molecular Biology (Methods and Protocols)*. Humana Press, pp. 63–70. [https://doi.org/10.1007/978-1-60327-198-1\\_6](https://doi.org/10.1007/978-1-60327-198-1_6).
- David, S., Bucchieri, F., Corrao, S., Czarnecka, A.M., Campanella, C., Farina, F., Peri, G., Tomasello, G., Sciumè, C., Modica, G., La Rocca, G., Anzalone, R., Giuffrè, M., De Macario, E.C., Macario, A.J.L.L., Cappello, F., Zummo, G., Conway De Macario, E., Macario, A.J.L.L., Cappello, F., Zummo, G., 2013. Hsp102: anatomic distribution, functions, and involvement in human disease. *Front. Biosci. Elit. 5* (E), 768–778. <https://doi.org/10.2741/E657>.
- Feliu, N., Kohonen, P., Ji, J., Zhang, Y., Karlsson, H.L., Palmberg, L., Nyström, A., Fadeel, B., 2015. Next-generation sequencing reveals low-dose effects of cationic dendrimers in primary human bronchial epithelial cells. *ACS Nano* 9, 146–163. <https://doi.org/10.1021/nn5061783>.
- Fernández Freire, P., Peropadre, A., Rosal, R., Pérez Martín, J.M., Hazen, M.J., 2015. Toxicological assessment of third generation (G3) poly (amidoamine) dendrimers using the *Allium cepa* test. *Sci. Total Environ.* <https://doi.org/10.1016/j.scitotenv.2015.07.137>.
- Gonzalo, S., Rodea-Palomares, I., Leganés, F., García-Calvo, E., Rosal, R., Fernández-Piñas, F., 2015. First evidences of PAMAM dendrimer internalization in microorganisms of environmental relevance: a linkage with toxicity and oxidative stress. *Nanotoxicology* 9, 706–718. <https://doi.org/10.3109/17435390.2014.969345>.
- Gusmão, D.S., Páscoa, V., Mathias, L., Vieira, I.J.C., Braz-Filho, R., Lemos, F.J.A., 2002. *Derris (Lonchocarpus) urucu* (Leguminosae) extract modifies the peritrophic matrix structure of *Aedes aegypti* (Diptera: Culicidae). *Mem. Inst. Oswaldo Cruz* 97, 371–375. <https://doi.org/10.1590/S0074-02762002000300017>.
- Heiden, T.C.K., Dengler, E., Kao, W.J., Heideman, W., Peterson, R.E., 2007. Developmental toxicity of low generation PAMAM dendrimers in zebrafish. *Toxicol. Appl. Pharmacol.* 225, 70–79. <https://doi.org/10.1016/j.taap.2007.07.009>.
- Herrero, O., Planelló, R., Gómez-Sande, P., Aquilino, M., Morcillo, G., 2014. Evaluation of the toxic effects of phthalates on natural populations of *Chironomus riparius* (Diptera): implications for ecotoxicity studies. *Rev. Toxicol.* 31, 176–186.
- Herrero, O., Planelló, R., Morcillo, G., 2015. The plasticizer benzyl butyl phthalate (BBP) alters the ecdysone hormone pathway, the cellular response to stress, the energy metabolism, and several detoxication mechanisms in *Chironomus riparius* larvae. *Chemosphere* 128, 266–277. <https://doi.org/10.1016/j.chemosphere.2015.01.059>.
- Herrero, O., Planelló, R., Morcillo, G., 2016. The ribosome biogenesis pathway as an early target of benzyl butyl phthalate (BBP) toxicity in *Chironomus riparius* larvae. *Chemosphere* 144, 1874–1884. <https://doi.org/10.1016/j.chemosphere.2015.10.051>.
- Herrero, O., Aquilino, M., Sánchez-Argüello, P., Planelló, R., 2018. The BPA-substitute bisphenol S alters the transcription of genes related to endocrine, stress response and biotransformation pathways in the aquatic midge *Chironomus riparius* (Diptera, Chironomidae). *PLoS One* 13, e0193387. <https://doi.org/10.1371/journal.pone.0193387>.
- Jain, K., Kesharwani, P., Gupta, U., Jain, N.K., 2010. Dendrimer toxicity: let's meet the challenge. *Int. J. Pharm.* 394, 122–142. <https://doi.org/10.1016/j.ijpharm.2010.04.027>.
- Janaszewska, A., Mączyska, K., Matuszko, G., Appelhans, D., Voit, B., Klajnert, B., Bryszewska, M., 2012. Cytotoxicity of PAMAM, PPI and maltose modified PPI dendrimers in Chinese hamster ovary (CHO) and human ovarian carcinoma (SKOV3) cells. *New J. Chem.* 36, 428–437. <https://doi.org/10.1039/C1NJ20489K>.
- Janaszewska, A., Lazniewska, J., Trzepiński, P., Marcinkowska, M., Klajnert-Maculewicz, B., 2019. Cytotoxicity of dendrimers. *Biomolecules*. <https://doi.org/10.3390/biom9080330>.
- Kavyani, S., Amjad-Iranagh, S., Modarress, H., 2014. Aqueous poly(amidoamine) dendrimer G3 and G4 generations with several interior cores at pHs 5 and 7: a molecular dynamics simulation study. *J. Phys. Chem. B* 118, 3257–3266. <https://doi.org/10.1021/jp409195c>.
- King, A.M., MacRae, T.H., 2015. Insect heat shock proteins during stress and diapause. *Annu. Rev. Entomol.* 60, 59–75. <https://doi.org/10.1146/annurev-ento-011613-162107>.
- Kunzmann, A., Andersson, B., Thurnherr, T., Krug, H., Scheynius, A., Fadeel, B., 2011. Toxicology of engineered nanomaterials: focus on biocompatibility, biodistribution and biodegradation. *Biochim. Biophys. Acta* 1810, 361–373. <https://doi.org/10.1016/j.bbagen.2010.04.007>.
- Li, J., Liang, H., Liu, J., Wang, Z., 2018. Poly (amidoamine) (PAMAM) dendrimer mediated delivery of drug and pDNA/siRNA for cancer therapy. *Int. J. Pharm.* 546, 215–225. <https://doi.org/10.1016/j.ijpharm.2018.05.045>.
- Liao, W., McNutt, M.A., Zhu, W.-G., 2009. The comet assay: a sensitive method for detecting DNA damage in individual cells. *Methods* 48, 46–53. <https://doi.org/10.1016/j.ymeth.2009.02.016>.
- Lu, X., Liu, Y., Kong, X., Lobie, P.E., Chen, C., Zhu, T., 2013. Nanotoxicity: a growing need for study in the endocrine system. *Small* 9, 1654–1671. <https://doi.org/10.1002/smll.201201517>.
- Mantilla, J.G., Gomes, L., Cristancho, M.A., 2017. The differential expression of *Chironomus* spp genes as useful tools in the search for pollution biomarkers in freshwater ecosystems. *Brief. Funct. Genomics* 86, 377–384. <https://doi.org/10.1093/bfpg/elix021>.
- Martinez, C.S., Igartúa, D.E., Calienni, M.N., Feas, D.A., Siri, M., Montanari, J., Chiamoni, N.S., Alonso, S. del V., Prieto, M.J., 2017. Relation between biophysical properties of nanostructures and their toxicity on zebrafish. *Biophys. Rev.* 9, 775–791. <https://doi.org/10.1007/s12551-017-0294-2>.
- Martín-Folgar, R., de la Fuente, M., Morcillo, G., Martínez-Guitarte, J.-L., 2015. Characterization of six small HSP genes from *Chironomus riparius* (Diptera, Chironomidae): differential expression under conditions of normal growth and heat-induced stress. *Comp. Biochem. Physiol. A Mol. Integr. Physiol.* 188, 76–86. <https://doi.org/10.1016/j.cbpa.2015.06.023>.
- Maynard, J.C., Pham, T., Zheng, T., Jockheck-Clark, A., Rankin, H.B., Newgard, C.B., Spana, E.P., Nicchitta, C.V., 2010. Gp93, the *Drosophila* GRP94 ortholog, is required for gut epithelial homeostasis and nutrient assimilation-coupled growth control. *Dev. Biol.* 339, 295–306. <https://doi.org/10.1016/j.ydbio.2009.12.023>.
- Mecke, A., Lee, D.-K., Ramamoorthy, A., Orr, B.G., Banaszak Holl, M.M., 2005. Synthetic and natural polymeric polymer nanoparticles interact selectively with fluid-phase domains of DMPC lipid bilayers. *Langmuir* 21, 8588–8590. <https://doi.org/10.1021/la051800w>.
- de Melo, M.S., Nazari, E.M., Müller, Y.M.R., Gismondini, E., 2020. Modulation of antioxidant gene expressions by Roundup® exposure in the decapod *Macrobrachium potiuna*. *Ecotoxicol. Environ. Saf.* 190, 110086. <https://doi.org/10.1016/j.ecoenv.2019.110086>.
- Mintzer, M.A., Grinstaff, M.W., 2011. Biomedical applications of dendrimers: a tutorial. *Chem. Soc. Rev.* 40, 173–190. <https://doi.org/10.1039/B901839P>.

- Mortimer, M., Kasemets, K., Heinlaan, M., Kurvet, I., Kahru, A., 2008. High throughput kinetic *Vibrio fischeri* bioluminescence inhibition assay for study of toxic effects of nanoparticles. *Toxicol. in Vitro* 22, 1412–1417. <https://doi.org/10.1016/j.tiv.2008.02.011>.
- Mukherjee, S.P., Davoren, M., Byrne, H.J., 2010a. *In vitro* mammalian cytotoxicological study of PAMAM dendrimers - towards quantitative structure activity relationships. *Toxicol. in Vitro* 24, 169–177. <https://doi.org/10.1016/j.tiv.2009.09.014>.
- Mukherjee, S.P., Lyng, F.M., Garcia, A., Davoren, M., Byrne, H.J., 2010b. Mechanistic studies of *in vitro* cytotoxicity of poly(amidoamine) dendrimers in mammalian cells. *Toxicol. Appl. Pharmacol.* 248, 259–268. <https://doi.org/10.1016/j.taap.2010.08.016>.
- Naha, P., Mukherjee, S., Byrne, H., 2018. Toxicology of engineered nanoparticles: focus on poly(amidoamine) dendrimers. *Int. J. Environ. Res. Public Health* 15, 338. <https://doi.org/10.3390/ijerph15020338>.
- Naha, P.C., Byrne, H.J., 2013. Generation of intracellular reactive oxygen species and genotoxicity effect to exposure of nanosized polyamidoamine (PAMAM) dendrimers in PLHC-1 cells *in vitro*. *Aquat. Toxicol.* 132–133, 61–72. <https://doi.org/10.1016/j.aquatox.2013.01.020>.
- Naha, P.C., Davoren, M., Casey, A., Byrne, H.J., 2009. An ecotoxicological study of poly(amidoamine) dendrimers-toward quantitative structure activity relationships. *Environ. Sci. Technol.* 43, 6864–6869. <https://doi.org/10.1021/es901017v>.
- Nicholls, C., Li, H., Liu, J.-P., 2012. GAPDH: a common enzyme with uncommon functions. *Clin. Exp. Pharmacol. Physiol.* 39, 674–679. <https://doi.org/10.1111/j.1440-1681.2011.05599.x>.
- OECD, 2004. Test No. 219: Sediment-water Chironomid Toxicity Test Using Spiked Water. Organisation for Economic Co-operation and Development, Paris.
- OECD, 2010. List of Manufactured Nanomaterials and List of Endpoints for Phase One of the Sponsorship Programme for the Testing of Manufactured Nanomaterials. OECD Series on the Safety of Manufactured Nanomaterials. Number 27. Organisation for Economic Co-operation and Development, Paris.
- OECD, 2011. Test No. 235: Chironomus sp., Acute Immobilisation Test. Organisation for Economic Co-operation and Development, Paris.
- Oliveira, E., Casado, M., Faria, M., Soares, A.M.V.M., Navas, J.M., Barata, C., Piña, B., 2014. Transcriptomic response of zebrafish embryos to polyaminoamine (PAMAM) dendrimers. *Nanotoxicology* 8, 92–99. <https://doi.org/10.3109/17435390.2013.858376>.
- Petit, A.-N., Eullaffroy, P., Debenest, T., Gagné, F., 2010. Toxicity of PAMAM dendrimers to *Chlamydomonas reinhardtii*. *Aquat. Toxicol.* 100, 187–193. <https://doi.org/10.1016/j.aquatox.2010.01.019>.
- Petit, A.-N., Debenest, T., Eullaffroy, P., Gagné, F., 2012. Effects of a cationic PAMAM dendrimer on photosynthesis and ROS production of *Chlamydomonas reinhardtii*. *Nanotoxicology* 6, 315–326. <https://doi.org/10.3109/17435390.2011.579628>.
- Planelló, R., Martínez-Guitarte, J.L., Morcillo, G., 2010. Effect of acute exposure to cadmium on the expression of heat-shock and hormone-nuclear receptor genes in the aquatic midge *Chironomus riparius*. *Sci. Total Environ.* 408, 1598–1603. <https://doi.org/10.1016/j.scitotenv.2010.01.004>.
- Planelló, R., Herrero, Ó., Gómez-Sande, P., Ozáez, I., Cobo, F., Servia, M.J., 2015a. Ecdysone-related biomarkers of toxicity in the model organism *Chironomus riparius*: stage and sex-dependent variations in gene expression profiles. *PLoS One* 10, e0140239. <https://doi.org/10.1371/journal.pone.0140239>.
- Planelló, R., Servia, M.J., Gómez-Sande, P., Herrero, Ó., Cobo, F., Morcillo, G., 2015b. Transcriptional responses, metabolic activity and mouthpart deformities in natural populations of *Chironomus riparius* larvae exposed to environmental pollutants. *Environ. Toxicol.* 30, 383–395. <https://doi.org/10.1002/tox.21893>.
- Planelló, R., Herrero, O., García, P., Beltrán, E.M., Llorente, L., Sánchez-Argüello, P., 2020. Developmental/reproductive effects and gene expression variations in *Chironomus riparius* after exposure to reclaimed water and its fortification with carbamazepine and triclosan. *Water Res.* 178, 115790. <https://doi.org/10.1016/j.watres.2020.115790>.
- Procópio, T.F., Fernandes, K.M., Pontual, E.V., Ximenes, R.M., de Oliveira, A.R.C., Souza, C. de S., Melo, A.M.M. de A., Navarro, D.M.D.A.F., Paiva, P.M.G., Martins, G.F., Napoleão, T.H., 2015. *Schinus terebinthifolius* leaf extract causes midgut damage, interfering with survival and development of *Aedes aegypti* larvae. *PLoS One* 10, e0126612. <https://doi.org/10.1371/journal.pone.0126612>.
- Pryor, J.B., Harper, B.J., Harper, S.L., 2014. Comparative toxicological assessment of PAMAM and thiophosphoryl dendrimers using embryonic zebrafish. *Int. J. Nanomedicine* 9, 1947–1956. <https://doi.org/10.2147/IJN.S60220>.
- Santiago-Morales, J., Rosal, R., Hernando, M.D., Ulaszewska, M.M., García-Calvo, E., Fernández-Alba, A.R., 2014. Fate and transformation products of amine-terminated PAMAM dendrimers under ozonation and irradiation. *J. Hazard. Mater.* 266, 102–113. <https://doi.org/10.1016/j.jhazmat.2013.12.021>.
- Solary, E., Garrido, C., 2002. The forgotten chaperones. *Nat. Cell Biol.* 4, E125. <https://doi.org/10.1038/ncb0502-e125>.
- Suarez, I.J., Rosal, R., Rodríguez, A., Ucles, A., Fernández-Alba, A.R., Hernando, M.D., García-Calvo, E., 2011. Chemical and ecotoxicological assessment of poly(amidoamine) dendrimers in the aquatic environment. *TrAC Trends Anal. Chem.* 30, 492–506. <https://doi.org/10.1016/j.trac.2010.11.009>.
- Taenzler, V., Bruns, E., Dorgerloh, M., Pfeifle, V., Weltje, L., 2007. Chironomids: suitable test organisms for risk assessment investigations on the potential endocrine disrupting properties of pesticides. *Ecotoxicology* 16, 221–230. <https://doi.org/10.1007/s10646-006-0117-x>.
- Tamayo-Belda, M., González-Pleiter, M., Pulido-Reyes, G., Martín-Betancor, K., Leganés, F., Rosal, R., Fernández-Piñas, F., 2019. Mechanism of the toxic action of cationic G5 and G7 PAMAM dendrimers in the cyanobacterium: *Anabaena* sp. PCC7120. *Environ. Sci. Nano* 6, 863–878. <https://doi.org/10.1039/c8en01409d>.
- Tristan, C., Shahani, N., Sedlak, T.W., Sawa, A., 2011. The diverse functions of GAPDH: views from different subcellular compartments. *Cell. Signal.* 23, 317–323. <https://doi.org/10.1016/j.cellsig.2010.08.003>.
- Truman, J.W., 2019. The evolution of insect metamorphosis. *Curr. Biol.* 29, R1252–R1268. <https://doi.org/10.1016/j.cub.2019.10.009>.
- Ulaszewska, M.M., Hernando, M.D., Uclés, A., Rosal, R., Rodríguez, A., García-Calvo, E., Fernández-Alba, A.R., 2012. Chemical and ecotoxicological assessment of dendrimers in the aquatic environment. *Comprehensive Analytical Chemistry*. Elsevier B.V., pp. 197–233. <https://doi.org/10.1016/B978-0-444-56328-6.00006-2>.
- Uram, Ł., Szuster, M., Filipowicz, A., Gargas, K., Wołowicz, S., Wałajczyk-Rode, E., 2015. Different patterns of nuclear and mitochondrial penetration by the G3 PAMAM dendrimer and its biotin-pyridoxal bioconjugate BC-PAMAM in normal and cancer cells *in vitro*. *Int. J. Nanomedicine* 10, 5647–5661. <https://doi.org/10.2147/IJN.S87307>.
- USEPA, 2000. *Methods for Measuring the Toxicity and Bioaccumulation of Sediment-associated Contaminants With Freshwater Invertebrates*. Second edition. U.S. Environmental Protection Agency, Washington.
- Vandesompele, J., De Preter, K., Pattyn, F., Poppe, B., Van Roy, N., De Paepe, A., Speleman, F., 2002. Accurate normalization of real-time quantitative RT-PCR data by geometric averaging of multiple internal control genes. *Genome Biol.* 3. <https://doi.org/10.1186/gb-2002-3-7-research0034> research0034.1.
- Walczyńska, M., Jakubowski, W., Wasiaś, T., Kadziola, K., Bartoszek, N., Kotarba, S., Siatkowska, M., Komorowski, P., Walkowiak, B., 2018. Toxicity of silver nanoparticles, multiwalled carbon nanotubes, and dendrimers assessed with multicellular organism *Caenorhabditis elegans*. *Toxicol. Mech. Methods* 28, 432–439. <https://doi.org/10.1080/15376516.2018.1449277>.
- Zhang, L., Yang, J., Li, H., You, J., Chatterjee, N., Zhang, X., 2020. Development of the transcriptome for a sediment ecotoxicological model species, *Chironomus dilutus*. *Chemosphere* 244, 125541. <https://doi.org/10.1016/j.chemosphere.2019.125541>.